

Structural Dynamics of Myoglobin Probed by Femtosecond Infrared Spectroscopy of the Amide Band

Seongheun Kim, Geunyoung Jin, and Manho Lim*

Department of Chemistry and Chemistry Institute for Functional Materials, Pusan National University, Busan 609-735, Korea
Received July 22, 2003

The dynamics of the tertiary conformation of myoglobin (Mb) after photolysis of carbon monoxide was investigated at 283 K solution by probing amide I and II bands using femtosecond IR absorption spectroscopy. Time-resolved spectra in the amide region evolve with 6-12 ps time scale without noticeable subpicosecond dynamics. The spectra measured at 100 ps delay after photolysis is similar to the difference FTIR spectrum at equilibrium. Time-resolved spectra of photoexcited Mb evolve modestly and their amplitudes are less than 8% of those of photolyzed MbCO, indicating that thermal contribution to the spectral evolution in the amide region is negligible. These observations suggest that the conformational relaxation ensuing photolysis of MbCO be complex and the final deoxy protein conformation have been substantially formed by 100 ps, probably with 6-12 ps time constant.

Key Words : Conformational relaxation, Myoglobin, Femtosecond infrared spectroscopy, MbCO

Introduction

A full understanding of protein function requires a detailed knowledge of the relation between structural and dynamical properties. Myoglobin (Mb) that reversibly binds small ligands such as O₂, CO, or NO, has long served as a model system for the experimental and theoretical investigation of protein dynamics and its relation to structure and function.¹ X-ray diffraction studies have shown that the structures of ligated Mb and de-ligated Mb (dMb) differ.²⁻⁴ The loss of a ligand from ligated Mb triggers a conformational change that alters the ligand binding properties of the protein. This conformational transition eventually leads to a change in the quaternary conformation of hemoglobin (a tetrameric protein with subunits similar in structure to Mb), resulting in its cooperative binding of ligands, the allosteric control mechanism of O₂ binding efficiency.⁵ For example, dissociation of CO from carbonmonoxy Mb (MbCO) generates dMb in the MbCO conformation (Mb*) and triggers specific conformational relaxation associated with the transition from MbCO to Mb.

MbCO has been a favorable sample in time-resolved spectroscopic studies because it exhibits high chemical stability in solution, ultrafast (<50 fs) photolyzability by visible pulse,⁶ almost unit quantum efficiency for photolysis,⁷ and little geminate recombination of photolyzed CO.⁸ Photodissociation of MbCO and its ensuing dynamics as fast as a femtosecond time scale have been studied by numerous time-resolved spectroscopic methods including uv-vis absorption,^{6,9} time-resolved circular dichroism,¹⁰ time-resolved infrared,^{11,12} time-resolved resonance Raman,¹³ and transient grating.^{14,15} Majority of these studies have focused on motion of the ligand or the heme, due largely to its conven-

ient absorbances. Direct probe of protein response has been rarely realized. Information on the protein itself is indirectly inferred from measurements on the strongly absorbing heme or bound CO. Recently a number of time-resolved X-ray crystallographic studies up to 150 ps time resolution have been carried out to monitor the protein motion after photolysis of MbCO.¹⁶⁻¹⁸ While time-resolved crystallography reveals the frame-by-frame structural evolution of the protein at an atomistic level, it cannot assess protein dynamics under physiologically relevant conditions where thermally driven, functionally important conformational fluctuations can occur. New insight into function of the protein obtained by time-resolved crystallography need to be supplemented by spectroscopic investigations of a protein on the relevant time scales in physiologically relevant conditions.¹⁸

Vibrational spectra in the amide region of a protein are known to be a sensitive probe into its secondary structure.¹⁹⁻²¹ The amide region of the spectra has been used to quantitatively predict secondary structures of the protein.¹⁹⁻²¹ Due to recent advances in time-resolved IR spectroscopy,^{22,23} IR changes in the amide spectral region on ultrashort time scales can be readily measured, enabling us to directly probe protein motions arising from conformational changes. In contrast to methods probing heme absorption such as time-resolved resonance Raman and circular dichroism, time-resolved IR spectroscopy can directly observe changes in protein structure with minimal interference from the heme.^{11,12,24} Even though the amide band consists of a large number of overlapping absorbances, time-resolved IR spectroscopy can resolve a subtle change in the band resulting from the photolytic perturbation and supply information on the functional changes isolated from the large static background because it measures the pump-induced change. Therefore, time-resolved IR spectroscopy in the amide region is a powerful tool for studying the protein dynamics coupled to photolysis of ligated heme protein.^{24,25}

*To whom correspondence should be addressed. E-mail: mhlim@pusan.ac.kr

Most of the previous time-resolved IR spectroscopy on heme proteins have probed the bound CO near 1950 cm^{-1} and the photolyzed CO trapped in the heme pocket near 2100 cm^{-1} , providing a detailed knowledge on the dynamics of ligand motion and recombination processes.^{11,12} There has been a picosecond IR spectroscopy work in the amide I band centered about 1650 cm^{-1} probing the dynamics of protein motion after photolysis of MbCO.²⁴ Here we report the use of time-resolved IR spectroscopy in the amide I and II region on a femtosecond time scale to extend its utility in direct investigation of protein dynamics.

Materials and Methods

Sample Preparation. A 15 mM dMb was prepared by dissolving lyophilized skeletal horse Mb (Sigma) in deoxygenated D_2O buffered with 0.1 M potassium phosphate (pD 7.4), reducing with 2 equivalent concentration of freshly prepared sodium dithionite (Aldrich). MbCO was obtained by bubbling CO gas (Matheson) to the dMb sample for 20 min. All sample preparation was carried out at ice bath to minimize thermal denature. To remove light scattering sources such as dust particles and denatured protein aggregates, all samples were filtered through a $5\text{-}\mu\text{m}$ membrane filter before loading in a gas-tight $6\text{-}\mu\text{m}$ -path-length sample cell with 2-mm-thick CaF_2 windows. During data collection the sample cell was rotated sufficiently fast so that each photolyzing laser pulse illuminated a fresh volume of the sample. The temperature of the rotating sample cell was $283 \pm 1\text{ K}$. Throughout the experiments the integrity and concentration of sample was routinely checked using uv-vis and FT-IR spectroscopy. Because water is a strong IR absorber, the sample was prepared in D_2O to isotopically shift interested spectrum into a region with greater IR transmission.

The Femtosecond Mid-IR Spectrometer. The details of the time-resolved mid-IR spectrometer will be described elsewhere. Briefly, a commercial Ti:sapphire oscillator/amplifier system (Hurricane, Spectra Physics, CA) is used to generate 110 fs pulses at 800 nm with an energy of $700\text{ }\mu\text{J}$ at a repetition rate of 1 kHz. Two identical home-built optical parametric amplifiers (OPA), pumped by the amplified pulse, are used to generate visible pump pulse²⁶ and mid-IR probe pulse.^{22,23} In a double-pass OPA setup, a single filament white light produced in a 1-mm-thick sapphire window seeds a 4-mm-thick type-II BBO crystal, pumped with $3\text{ }\mu\text{J}$ for the first pass and $200\text{ }\mu\text{J}$ for the second pass. The OPA produces near transform-limited 70-100 fs pulses, tunable between 1.16 and $2.58\text{ }\mu\text{m}$, with a total energy of $50\text{ }\mu\text{J}$ in the signal and idler pulse. To generate tunable pump pulse in the visible region, the signal pulse of one OPA is separated from its idler in a dichroic beamsplitter and frequency doubled in a type-I, 1-mm-thick BBO crystal.²⁶ The signal and idler pulse of the other OPA are difference frequency mixed in a 1.5-mm-thick, type-I AgGaS_2 crystal to yield tunable mid-IR probe pulse with duration of 110 fs.²² Mid-IR pulse with a typical spectral bandwidth of 160

cm^{-1} and $1\text{ }\mu\text{J}$ of energy is collected by a curved mirror, filtered by a long pass filter (FXLP-0300, Janos Technology, VT), and a small portion of the mid-IR pulse is reflected by a wedged BaF_2 -window. The visible pump pulse set at 580 nm with $3\text{ }\mu\text{J}$ of energy, optically delayed by a computer controlled translational stage (Nanomotion II, Melles Griot, CA), photoexcites or photolyzes the sample and its transient mid-IR absorbance is measured with the probe pulse. The polarization of the pump pulse was set at the magic angle (54.7°) relative to the probe pulse to recover isotropic absorption spectrum.

The broadband transmitted probe pulse is detected with a $\text{N}_2(l)$ -cooled HgCdTe array detector (Infrared Associates, FL) which consists of 64 elements (0.4 mm high, 0.2 mm wide) with the typical peak detectivity, $D^* = 2 \times 10^{10}\text{ cm Hz}^{1/2}\text{ W}^{-1}$ at 10 kHz. The array detector is mounted on the focal plane of a 320 mm IR monochromator (Triax320, Horiba, NJ) with a 150 l/mm grating, resulting in a spectral resolution of *ca.* $1.1\text{ cm}^{-1}/\text{pixel}$ at 1600 cm^{-1} . The signals from each of the detector elements were amplified with a home-built 64-channel amplifier and digitized by a 12-bit analog-to-digital converter (PCI6071E, National Instruments). The transient spectra spanning 140 cm^{-1} are a superposition of two 64-point spectra that overlap by a few elements. The monochromator was calibrated against rovibrational spectral lines of water vapor in the same spectra region investigated. The pump-induced change in the absorbance of the sample ΔA , is determined by chopping the pump pulse at half the repetition frequency of the laser and computing the difference between the pumped and unpumped absorbance. Chopping the excitation light pulse afforded greater immunity to long-term instrumental drift. Due to the excellent short-term stability of the IR light source ($<1\%$ rms), less than 1×10^{-4} rms in absorbance units after 0.5 sec of signal averaging is routinely obtained without single shot referencing with an independent detector. The pump spot ($180\text{ }\mu\text{m}$ diameter) was made larger than the probe spot ($120\text{ }\mu\text{m}$ diameter) to ensure spatially uniform photoexcitation across the spatial dimensions of the probe pulse.²⁷ Moderate pump energy with decent beam size also minimizes extended thermal effects. Time resolution attained in this work, determined by transient absorption of Si wafer, is $<180\text{ fs}$ full width at half maximum.

Results and Discussion

The equilibrium FT-IR spectra of dMb and MbCO in D_2O solution at room temperature, shown in Figure 1, are almost identical except the band at 1943 cm^{-1} resulting from the CO stretching mode of MbCO. However, as shown in Figure 2(a), the difference in conformation between de-ligated and ligated Mb results in small spectral features ($\pm 4 \times 10^{-3}$ out of 0.8 in absorbance units) in the amide I ($1700\text{-}1600\text{ cm}^{-1}$) and amide II ($1600\text{-}1500\text{ cm}^{-1}$) region in the difference spectrum (dMb minus MbCO). The major spectral features in the difference spectrum occur in the amide I region, in particular a negative-going feature at 1665 cm^{-1} and a

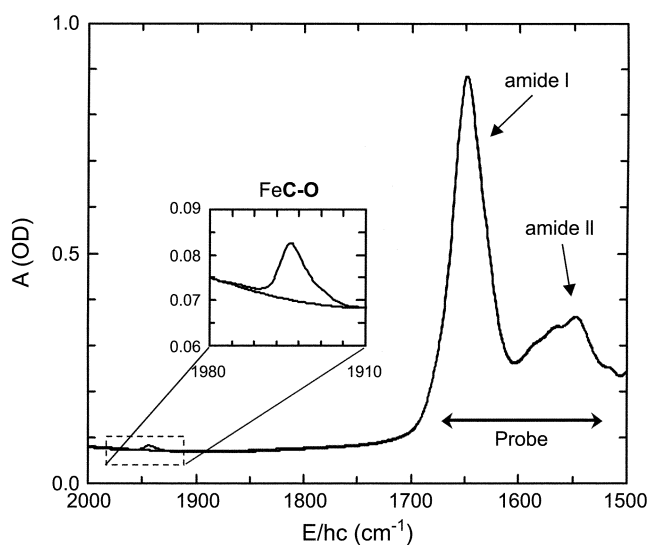


Figure 1. Equilibrium FTIR spectra of 15 mM dMb and MbCO. Both spectra are overlapped except a band at 1943 cm^{-1} . Inset is an expanded view of the CO stretching mode of MbCO. Probe with an arrow depicts spectral region investigated. OD; optical density.

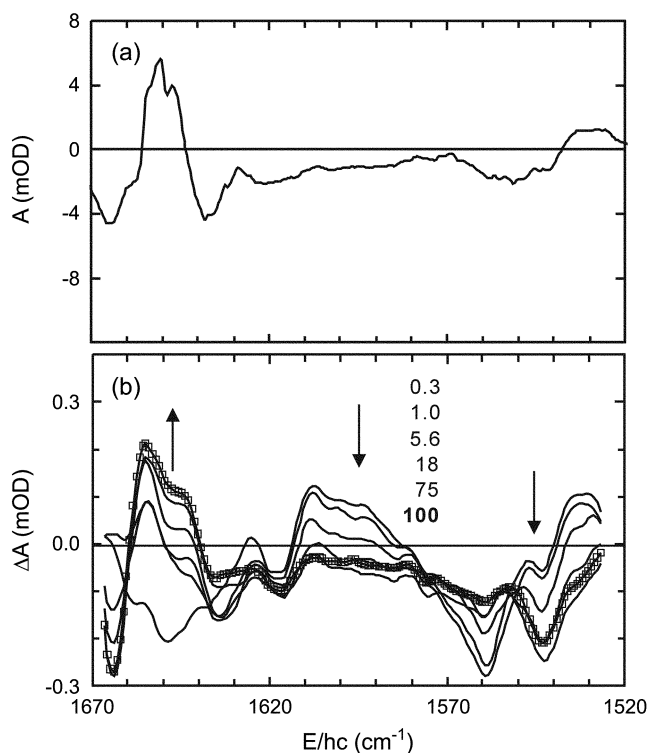


Figure 2. (a) The difference spectrum in the amide region obtained by subtracting MbCO spectrum from dMb spectrum. (b) Representative time resolved mid-IR spectra of photodissociated MbCO over the spectral range $1670\text{--}1520\text{ cm}^{-1}$. Pump-probe delays are 0.3 ps, 1 ps, 5.6 ps, 18 ps, 75 ps, and 100 ps in the direction of the arrows. The spectrum at 100 ps delay is shown with symbols for better distinction. mOD; mili-OD.

positive-going feature at 1650 cm^{-1} . There are also observable spectral features in the amide II band, mainly a negative-going feature at 1544 cm^{-1} . The difference spectrum in the amide I band is similar to the previous observation by

Causgrove *et al.*²⁵

The transient IR spectra near 1940 cm^{-1} after photolysis of MbCO (data not shown) reveal a negative-going feature arising from the loss of the bound CO. The magnitude of the bleach corresponds to $\sim 15\%$ photolysis of MbCO. The bleach appears faster than the resolution of the instrument, consistent with ultrafast photodissociation of CO inferred from the appearance of a deoxy-like Soret band absorption spectrum within 50 fs.⁶ The instantaneous bleach of the bound CO has already been observed in CO-ligated heme proteins by fs IR spectroscopy.¹¹ The bleach maintains its magnitude for 100 ps, the time window of the present experiment. This is in agreement with the expected recombination ($<0.1\%$) from the exponential geminate rebinding process with a yield of 3.7% and a rebinding rate coefficient of $(180\text{ ns})^{-1}$, the values reported for aqueous MbCO.⁸

Time resolved mid-IR spectra of photodissociated MbCO were collected over the spectral range $1670\text{--}1520\text{ cm}^{-1}$ and a few of them at representative times are shown in Figure 2(b). Data are shown for pump-probe delay times larger than 300 fs to avoid any contributions from truncated free induction decay of bound CO and from signals when pump-probe pulses are overlapped.^{28,29} At early times the time-resolved spectra are quite different from the difference spectrum at equilibrium but rapidly evolve toward the static difference spectrum. The photolyzed CO resides in the heme pocket during the time window of the present experiment, and thus the observed spectral evolution is influenced neither from its geminate rebinding nor escape from the heme pocket. The transient spectra start to show asymptotic behavior by 50 ps. The shape of the spectrum at 100 ps generally reproduces the main features of the static difference spectrum, although some differences can be seen. As shown in Figure 3, time-dependent behavior of the transient spectra can be clearly seen in several transient kinetic traces where the probe wavelengths correspond to large change in the time-resolved spectra. Since the photolyzed CO remains in the heme pocket for hundreds of nanoseconds,³⁰ time-resolved spectrum at 100 ps might be different from the difference spectrum at equilibrium. Furthermore, the conformational relaxation after photolysis of MbCO is highly nonexponential and spans several decades,⁹ the conformation of Mb* at 100 ps likely differs from that of dMb, resulting in some residual difference between two spectra. The transient kinetic traces in Figure 3 are well described by a single exponential function. The symbols correspond to the experimental data and the thick solid lines represent fits to the data with exponential rise or decay. The transient kinetic at 1665 cm^{-1} , where the largest change in the amide I region of the static difference spectrum occurs, decays with a time constant of 8.1 ps and that at 1544 cm^{-1} , where the largest change in the amide II region occurs, decays with a time constant of 9 ps. Other kinetic traces in the amide II region at 1608, 1560, and 1534 cm^{-1} , shown in Figure 3(b), decay or rise with time constants of 7.7 ps, 6 ps, and 11.9 ps, respectively.

Photolysis of MbCO deposits energy into the heme, raising its temperature. Time-resolved IR spectra of photoexcited

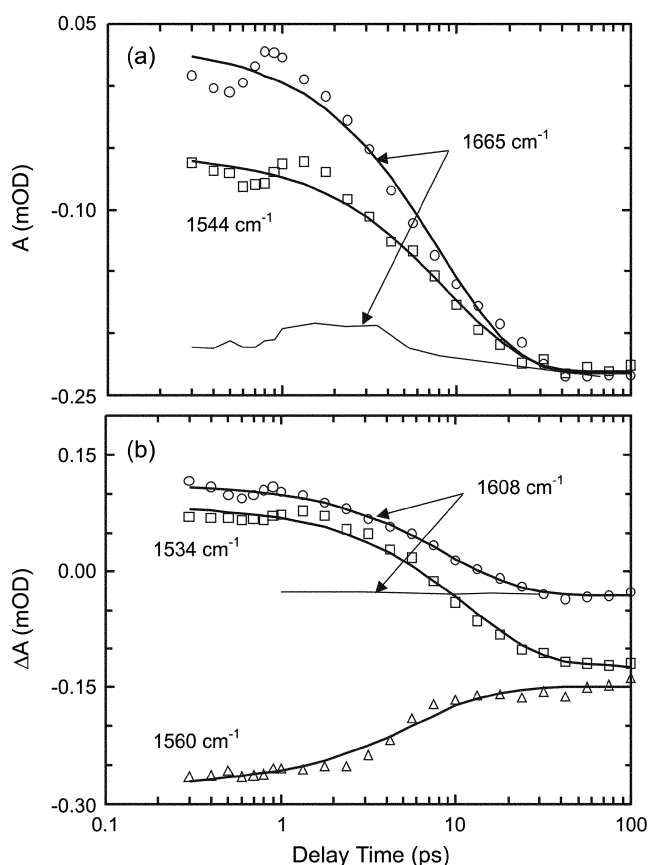


Figure 3. (a) Time-resolved IR absorption kinetic traces after photolysis of MbCO at 1665 cm^{-1} (open circles) and 1544 cm^{-1} (open squares). (b) Kinetic traces in the amide II region at 1608 cm^{-1} (open circles), 1560 cm^{-1} (open triangles), and 1534 cm^{-1} (open squares). The symbols correspond to the experimental data and the thick solid lines represent best fits to the data with exponential functions. Thin solid lines are transient kinetics of photoexcited Mb at characteristic wavelengths to estimate thermal contribution to the signal due to heating of the sample by the pump pulse.

Mb were obtained to account for signal due to heating of the sample by the pump pulse. Spectral evolution of amide band due to the heating is modest and the amplitudes of the transients of photoexcited Mb (thin solid lines in figure 3) are much smaller than those of MbCO. The energy deposited in the heme of MbCO can be estimated from our 580 nm photon energy (49 kcal/mol) minus the energy of the Fe-CO bond (16.2 kcal/mol)³¹ minus the reorganization of the protein (2.4 kcal/mol)³² minus the initial kinetic energy of the dissociated ligand (<20 kcal/mol).^{9,11} Depending on the initial kinetic energy of the dissociated ligand, as much as 62% of the pump photon energy can be added as excess thermal energy upon photolysis of MbCO. Thermal energy added to the heme is known to decay with 6 ps time scale,³³ similar to 6-12 ps time scale recovered in the transients of MbCO. However, the amplitudes of the transients of photoexcited Mb are less than 8% of those of photolyzed MbCO. Assuming that 62% of the amplitudes from the transients of photoexcited Mb are included in those of MbCO, the thermal contribution to the transients of MbCO

is at most 5% of the total amplitudes. Taking into account these observations, thermal contribution to the transients of MbCO is neglected. Causgrove *et al.* also argued that the transients observed after photolysis of MbCO are due to protein motion based on their measurements on temperature-dependent FTIR spectra of MbCO and D₂O solvent.²⁴

According to previous picosecond IR absorption measurement in the amide I band after photolysis of MbCO,²⁴ the band probed at 1666 cm^{-1} rises with 8.2 ps time constant and decays with 6.1 ps at 1656 cm^{-1} . The time resolved spectrum at 50 ps is generally the same as that at 1 μs which is almost identical to the difference spectrum at equilibrium,²⁵ suggesting that the majority of protein motion occurs within 50 ps. The kinetics of changes in the amide I region were also indistinguishable from the recombination kinetics measured at 1943 cm^{-1} , indicating that a conformational change occurs upon recombination and that the amide I band is a good marker for the conformational relaxation ensuing photolysis of MbCO.²⁵ While these measurements have focused on the amide I band and have a limited time-resolution, it established a foundation for this work. Here we have shown that the amide II band can also be utilized as a marker for the conformational change after photolysis of MbCO and there is no noticeable subpicosecond dynamics in protein structure.

The dynamics of the tertiary conformational change following photolysis of MbCO has been measured by probing the evolution of band III, a weak Fe-porphyrin charge-transfer band near 763 nm that is sensitive to the out-of-plane position of the Fe.^{9,34} This motion is highly nonexponential stretching over 5 decades in time, found to match the final phase of Fe out-of-plane displacement in MD simulations.³⁵ A recent transient grating experiment showed that protein-driven density waves develop on a 2 ps time scale after photolysis of MbCO.¹⁴ The density changes are suggested to correspond to a global tertiary conformational change of the protein. This fast density change is thought to arise from a collective displacement involving a large number of atoms in response to ligand dissociation. These kinds of experiments probing changes in heme absorption resulting from protein response to conformational changes are not uniquely sensitive to the protein response. On the contrary, time-resolved IR spectra in this experiment directly probe structural transition from a ligated to a deligated structure. Six to twelve picosecond recovered from the transients in amide band indicates that the majority of protein motion occurs in this time scale. The range of lifetime implies that protein motion is complex and cannot be represented by a single lifetime. The complexity of the motion is often manifested as nonexponential relaxation dynamics,^{9,35} which has been described as a conformational substates model.³⁶

In conclusion, we have measured the dynamics of the tertiary conformation of Mb at 283 K solution after photolysis of MbCO by probing amide I and II bands using femtosecond IR absorption spectroscopy. Time-resolved spectra in the amide region asymptotically approach to the

static difference spectrum with 6-12 ps time scale. The kinetics does not reveal any noticeable subpicosecond dynamics. Thermal contribution to the spectral evolution from excess photon energy is found to be negligible compared with the transient amplitudes of MbCO. These results suggest that the amide II band as well as amide I band be a good marker for the conformational change of Mb and majority of protein motion occur on 6-12 ps time scale.

Acknowledgement. This work was supported by grants from the Korea Science and Engineering Foundation through the Center for Integrated Molecular Systems (POSTECH). This research used femtosecond laser system in the Central Laboratory at Pusan National University. The authors would like to acknowledge the support of BK21 core program granted by Korea Research Foundation.

References

1. Springer, B. A.; Sligar, S. G.; Olson, J. S.; Phillips, G. N., Jr. *Chem. Rev.* **1994**, *94*, 699.
2. Kuriyan, J.; Wilz, S.; Karplus, M.; Petsko, G. A. *J. Mol. Biol.* **1986**, *192*, 133.
3. Phillips, S. E. V. *J. Mol. Biol.* **1980**, *142*, 531.
4. Takano, T. *J. Mol. Biol.* **1977**, *110*, 569.
5. Perutz, M. F.; Fermi, G.; Luisi, B.; Shaanan, B.; Liddington, R. C. *Acc. Chem. Res.* **1987**, *20*, 309.
6. Petrich, J. W.; Lambry, J. C.; Kuczera, K.; Karplus, M.; Poyart, C.; Martin, J. L. *Biochemistry* **1991**, *30*, 3975.
7. Gibson, Q. H.; Olson, J. S.; McKinnie, R. E.; Rohlfs, R. J. *J. Biol. Chem.* **1986**, *261*, 10228.
8. Henry, E. R.; Sommer, J. H.; Hofrichter, J.; Eaton, W. A. *J. Mol. Biol.* **1983**, *166*, 443.
9. Lim, M.; Jackson, T. A.; Anfinrud, P. A. *Proc. Natl. Acad. Sci. U. S. A.* **1993**, *90*, 5801.
10. Xie, X.; Simon, J. D. *Biochemistry* **1991**, *30*, 3682.
11. Anfinrud, P. A.; Han, C.; Hochstrasser, R. M. *Proc. Natl. Acad. Sci. U. S. A.* **1989**, *86*, 8387.
12. Lim, M.; Jackson, T. A.; Anfinrud, P. A. *Nature Struct. Biol.* **1997**, *4*, 209.
13. Findsen, E. W.; Friedman, J. M.; Ondrias, M. R.; Friedman, J. W. *Science* **1985**, *229*, 661.
14. Deak, J.; Chiu, H.; Lewis, C. M.; Miller, R. J. D. *J. Phys. Chem. B* **1998**, *102*, 6621.
15. Genberg, L.; Richard, L.; McLendon, G.; Miller, R. J. D. *Science* **1991**, *251*, 1051.
16. Brunori, M.; Vallone, B.; Cutruzzola, F.; Travaglini-Allocatelli, C.; Berendzen, J.; Chu, K.; Sweet, R. M.; Schlichting, I. *Proc. Natl. Acad. Sci. U. S. A.* **2000**, *97*, 2058.
17. Chu, K.; Vojtechovsky, J.; McMahon, B. H.; Sweet, R. M.; Berendzen, J.; Schlichting, I. *Nature* **2000**, *403*, 921.
18. Schott, F.; Lim, M.; Jackson, T. A.; Smirnov, A.; Soman, J.; Olson, J. S.; George, N.; Phillips, J.; Wulff, M.; Anfinrud, P. A. *Science* **2003**, *300*, 1944.
19. Dong, A.; Huang, P.; Caughey, W. S. *Biochemistry* **1990**, *29*, 3303.
20. Dong, A.; Huang, P.; Caughey, W. S. *Biochemistry* **1992**, *31*, 182.
21. Dousseau, F.; Pezolet, M. *Biochemistry* **1990**, *29*, 8771.
22. Hamm, P.; Lim, L.; Hochstrasser, R. M. *J. Phys. Chem. B* **1998**, *102*, 6123.
23. Hamm, P.; Kaindl, R. A.; Stenger, J. *Opt. Lett.* **2000**, *25*, 1798.
24. Causgrove, T. P.; Dyer, R. B. *J. Phys. Chem.* **1996**, *100*, 3273.
25. Causgrove, T. P.; Dyer, R. B. *Biochemistry* **1993**, *32*, 11985.
26. Lim, M.; Wolford, M. F.; Hamm, P.; Hochstrasser, R. M. *Chem. Phys. Lett.* **1998**, *290*, 355.
27. Lim, M. *Bull. Korean Chem. Soc.* **2002**, *23*, 865.
28. Hamm, P. *Chem. Phys.* **1995**, *200*, 415.
29. Wynne, K.; Hochstrasser, R. M. *Chem. Phys.* **1995**, *193*, 211.
30. Lim, M.; Jackson, T. A.; Anfinrud, P. A. *Science* **1995**, *269*, 962.
31. Rudolph, S. A.; Boyle, S. O.; Dresden, C. F.; Gill, S. J. *Biochemistry* **1972**, *11*, 1098.
32. Srajer, V.; Champion, P. M. *Biochemistry* **1991**, *30*, 7390.
33. Lim, M.; Jackson, T. A.; Anfinrud, P. A. *J. Phys. Chem.* **1996**, *100*, 12043.
34. Jackson, T. A.; Lim, M.; Anfinrud, P. A. *Chem. Phys.* **1994**, *180*, 131.
35. Kuczera, K.; Lambry, J. C.; Martin, J. L.; Karplus, M. *Proc. Natl. Acad. Sci. U. S. A.* **1993**, *90*, 5805.
36. Frauenfelder, H.; Parak, F.; Young, R. D. *Annu. Rev. Biophys. Chem.* **1988**, *17*, 451.